Electrical Power and Energy Systems 106 (2019) 232–241

Contents lists available at ScienceDirect

Electrical Power and Energy Systems

journal homepage: www.elsevier.com/locate/ijepes

Generation and transmission expansion planning with high penetration of wind farms considering spatial distribution of wind speed

Saeed Zolfaghari Moghaddam

Faculty of Electrical Engineering, Urmia University of Technology, Urmia, Iran

ARTICLE INFO

Keywords:
Poisson distribution
Scenario based optimal power flow
Simultaneous generation and transmission expansion planning
Spatial distribution of wind speed

ABSTRACT

This paper represents the effect of wind speed's spatial distribution on the simultaneous generation and transmission expansion planning of power systems including wind farms. To this end, wind farm's capacity factor is used as a practical parameter to model its output power. It is shown that ignoring wind speed's spatial distribution affects the expected exploitable wind power. In other words, the utilizable wind power of a wind farm in a power system would be overestimated if the spatial distribution of the wind speed is not considered and the wind farm's owner expects more utilizable wind power than what happens in the real world.

The objective function of the proposed mixed integer linear programming (MILP) model is to minimize total cost which includes three main parts: 1. The total investment cost of thermal generation units, transmission lines, and wind farms, 2. Expected operation cost of thermal generators, which is related to fuel consumption and penalty of the CO_2 emission, and 3. Expected loss cost of transmission lines. Furthermore, it is investigated that how different values of operation cost, as well as CO_2 emission tax, affect the proposed expansion planning model. Two test systems, namely IEEE 24-bus RTS and IEEE 118-bus test systems, are employed to evaluate the effectiveness of the proposed method. The results show that ignoring wind speed's spatial distribution not only changes the optimal plan but also makes the planner expect a further reduction in the value of objective function. This outcome is particularly true for high values of operation cost and emission taxes of greenhouse gases as well as high wind power penetration levels.

1. Introduction

The effects of power system expansion planning on continuous and reliable supply for electricity demand make it an important challenge for power system planners and researchers [1–3]. In this connection, wind power is one of the most promising renewable resources that have been used widely in the last decades in power systems [4,5]. The main disadvantage of wind energy is that wind power has stochastic variations [6]. Therefore, the more accurate modeling of the wind farm (WF)'s output power is, the more realistic solution for the power system expansion planning problem can be achieved. Many researchers have proposed transmission expansion planning (TEP) and/or generation expansion planning (GEP) with wind energy, either simultaneously or separately. In the related technical publications that consider wind power resources, only chronological (temporal) changes in wind speed have been taken into account. To model this feature of wind speed, different techniques such as time series method [7], k-nearest neighbor classification [8], neural networks [9], suitable probability distribution function [10], and other methods [11] have been used. Generally, it is assumed that at a certain time, the wind speed value in all places of a WF is the same. In [12], a bi-level programming model is proposed for coordinated planning of WF integration system and transmission network. A wind-thermal planning framework has been presented in [13], which examines the optimal expansion planning of gas-fired units to accommodate the uncertainty of wind generation. A flexible TEP method is introduced in [14], which takes into account the WF integration and demand response. Benders decomposition technique is another way used to solve TEP problem in the presence of wind energy [15,16]. In [17], a two-stage TEP methodology is proposed to minimize costs of investment and curtailed wind energy considering both normal and N-1 contingency conditions. In [18], a mixed integer linear programming formulation is proposed to minimize the installation cost of transmission lines, reactive power sources, and the annual operation cost of conventional generation. A tri-level reliability-constrained power system expansion planning model is presented in [19]. A generation expansion model is introduced in [4], which controls carbon dioxide (CO_2) emissions. Rajesh et al. [20] proposed a differential evolution algorithm to solve GEP problem with wind power plant. Ref. [21] proposes coordinated generation and transmission expansion planning in a deregulated electricity market considering WFs. The

E-mail address: s.zolfaghari@uut.ac.ir.

https://doi.org/10.1016/j.ijepes.2018.10.007
Received 23 August 2017; Received in revised form 17 July 2018; Accepted 6 October 2018

Nomenclature

Indices

t	indices of planning time period
i	indices of buses
cl	indices of candidate transmission lines
ctg	indices of candidate thermal generation units
cwf	indices of candidate wind farms
etg	indices of existent thermal generation units
el	indices of existent transmission lines
ls	indices of load scenarios

Parameters and constants

CL	total number of candidate transmission lines
CTG	total number of candidate thermal generation units
CWF	total number of candidate wind farms
ETG	total number of existent thermal generation units
EL	total number of existent transmission lines
T	total number of planning time horizon
LS	total number of load scenarios
$C_{t,cl}^{LI}$	investment cost of candidate line cl in planning time interval t ($)
$C_{t,ctg}^{TGI}$	investment cost of candidate thermal generator ctg in planning time interval t ($)
$C_{t,cwf}^{WBI}$	investment cost of a wind block of candidate wind farm cwf in planning time interval t ($)
ST	sub-periods of each planning time period (year)
OC_{etg}	operation cost of existent thermal generator etg ($/MWh)
OC_{ctg}	operation cost of candidate thermal generator ctg ($/MWh)
ER_{etg}	CO_2 emission rate of existent thermal generator etg (ton/MWh)
ER_{ctg}	CO_2 emission rate of candidate thermal generator ctg (ton/MWh)
$ETax$	CO_2 emission tax ($/ton)
CL_t^{pu}	cost of per unit loss ($/MWh)
α_{ls}	occurrence probability of load scenario ls
B_{ij}	susceptance of transmission line between buses i and j
G_{ij}	conductance of transmission line between buses i and j
$d_{t,i,ls}$	active load of bus i at time t in load scenario t
$ELCap_{\max,ij}$	maximum capacity of existent transmission line between buses i and j
$CLCap_{\max,ij}$	maximum capacity of candidate transmission line between buses i and j
$ETGCap_{\max,i,ng}$	maximum capacity of existent thermal generator etg (MW)
$CTGCap_{\max,i,ctg}$	maximum capacity of candidate thermal generator ctg (MW)
$ETGCap_{\min,i,ng}$	minimum capacity of existent thermal generator etg (MW)
$CTGCap_{\min,i,ctg}$	minimum capacity of candidate thermal generator ctg (MW)
CF_{cwf}	capacity factor of wind farm cwf
WBC	wind block capacity (MW)
dr	discount rate
$\delta_{\min,i}$	minimum voltage angle of bus i
$\delta_{\max,i}$	maximum voltage angle of bus i

Variables

$ul_{t,cl}$	binary variable that is equal 1 if candidate line cl is built in planning time interval t, and 0 otherwise
$ug_{i,t,ctg}$	binary variable that is equal 1 if candidate thermal generator ctg is built in bus i in planning time interval t, and 0 otherwise
$N_{i,t,cwf}^{WB}$	integer variable that shows the number of wind blocks of wind farm cwf that should be installed in bus i in planning time interval t
$P_{i,t,etg,ls}$	power generation of existent thermal generator etg in bus i, planning time interval t, and load scenario ls (MW)
$P_{i,t,ctg,ls}$	power generation of candidate thermal generator ctg in bus i, planning time interval t, and load scenario ls (MW)
$P_{cwf,i,t,ls}$	power generation of wind farm cwf in bus i, planning time interval t, and load scenario ls (MW)
$P_{el,t,ls}^{loss}$	power loss of existent line el in planning time interval t, and load scenario ls (MW)
$P_{el,t,ls}^{loss}$	power loss of candidate line cl in planning time interval t, and load scenario ls (MW)
$ELPF_{t,ij,ls}$	power flow of existent line from bus i to j in planning time interval t, and load scenario ls (MW)
$(CLPF_{t,ij,ls})$	power flow of candidate line from bus i to j in planning time interval t, and load scenario ls (MW)
$\delta_{t,i,ls}$	voltage angle of bus i in planning time interval t, and load scenario ls

Abbreviations

CF	capacity factor
GAMS	general algebraic modeling system
GEP	generation expansion planning
MCS	monte carlo simulation
MILP	mixed integer linear programming
OF	objective function
OPF	optimum power flow
TEP	transmission expansion planning
WF	wind farm
WT	wind turbine

uncertainty of the wind power is modeled using a normal distribution function while the particle swarm optimization (PSO) method is used to solve the presented nonlinear mixed-integer expansion problem. A new meta-heuristic method namely Imperialist Competitive Algorithm [22] is used to solve TEP problem in the presence of wind power. You et al. [23] proposed a method for the generation and transmission expansion co-optimization problem with a high wind power penetration. They proposed a scenario-based method to capture the variation and correlation of load and wind power. Ref. [24] develops a framework for transmission and wind power expansion planning as a bi-level optimization problem. It investigates the effect of TEP on private investment absorption for wind power expansion. A multistage optimization model is presented in [25] for generation expansion planning in which a quasi-exact solution approach is used to linearize the proposed model.

As previously mentioned, in all reviewed references, to apply the probabilistic nature of the WF into the power system expansion planning, only temporal changes of the wind speed have been considered; besides, it is assumed that the wind speed values in all locations of a WF are the same in a certain time. However, statistical spatial distribution of wind speed through WF is a key factor [26] that has not been considered in any of the existent expansion models of power systems including WFs. This paper evaluates the effect of wind speed's spatial distribution on the simultaneous GEP and TEP of power systems including WFs. For this purpose, both the statistical temporal distribution of wind speed and its statistical spatial distribution are considered to model the uncertainty of wind speed as much accurate as possible. Two test systems, namely IEEE 24-bus RTS and IEEE 118-bus, are employed to evaluate the effectiveness of the proposed method. The results show

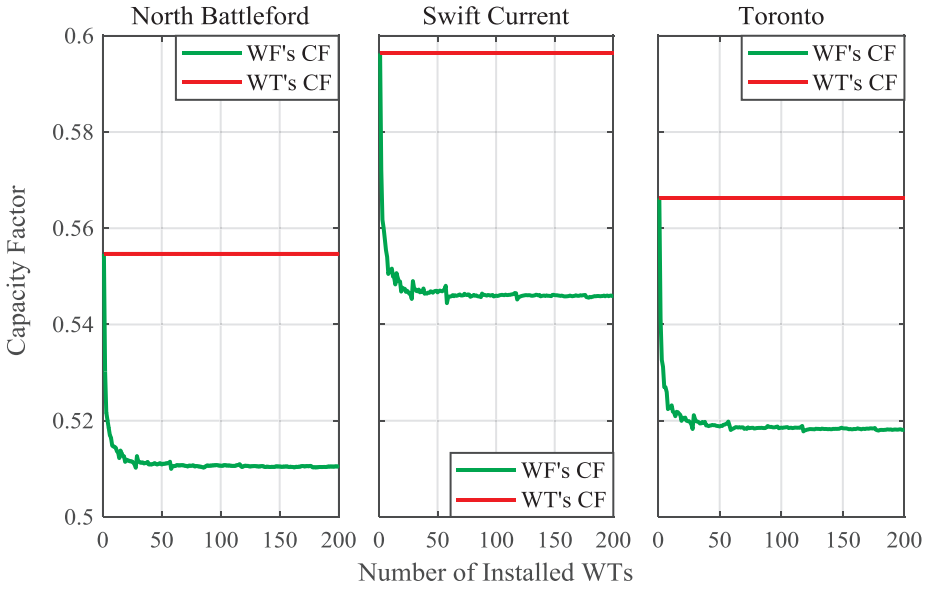

Fig. 1. WF's capacity factor versus the number of installed WTs.

Table 1
Main statistical characteristics of actual wind speed data.

Wind sites	Mean value (km/hour)	Standard deviation (km/hour)
North Battleford	14.625	9.59
Swift current	19.67	9.62
Toronto	17.22	10.56

that ignoring wind speed's spatial distribution not only changes the optimal plan but also makes the planner expect a further reduction in the value of objective function. This result is particularly true for high values of operation cost and emission taxes of greenhouse gases as well as high wind power penetration levels. The difference between estimated and actual wind power values could be unfavorable to both the WF's owner and the owner of energy storage systems that are widely used along with renewable energy sources [27]. This effect is especially important in competitive markets in which an accurate estimate of the wind power is critical. In addition, in most of the previous studies, the capacity of the WF is usually predetermined while in the proposed model, the optimal capacity of the WF is considered to be a decision variable.

The objective function of the proposed mixed integer linear programming (MILP) model is to minimize total cost including (1) The total investment cost of thermal generation units, transmission lines, and wind farms, (2) Expected operation cost of thermal generators, which is related to fuel consumption and penalty of the CO_2 emission, and (3) Expected loss cost of transmission lines. Two test systems, namely IEEE 24-bus and IEEE 118-bus, have been used to evaluate the effectiveness of the proposed method. It is observed that incorporating the wind speed's spatial distribution affects wind power penetration level and the optimal plan, which directly influences the objective of the simultaneous planning problem. This behavior is a vital issue especially in the future power systems in which renewable energy will be of particular importance.

The remainder of this paper is organized as follows. Section 2 introduces the main characteristics of the proposed model. Section 3 presents the problem formulation of the proposed simultaneous GEP and TEP. Test systems and their simulation results are given in Section 4. Eventually, the concluding remarks are discussed in Section 5.

2. Problem description

In this section, the main characteristics of the proposed model are explained. First, it is determined how to model the uncertainty of the WF's output power and load. Second, different parts of the proposed GEP and TEP model are described. Finally, the necessity of using probabilistic optimal power flow and its implementation procedure is presented.

2.1. WF's output power

The capacity factor (CF) of a wind turbine is defined as the ratio of its expected output power to its rated power [28]. Generally, the ratio of the expected output power of a wind farm to its rated power is known

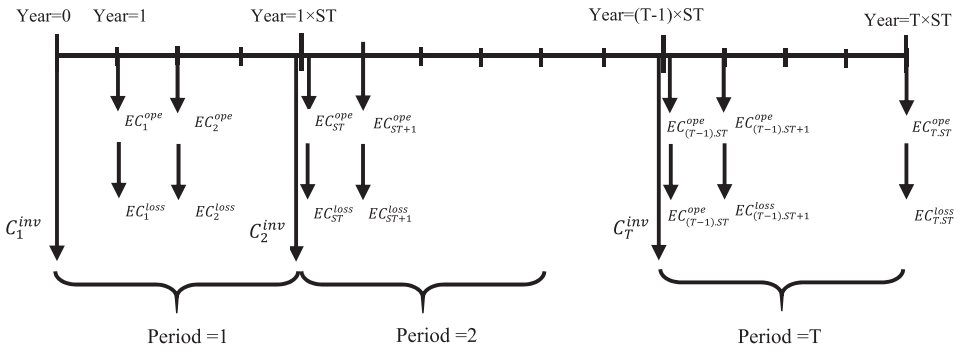

Fig. 2. Cash flow diagram of the power system expansion planning.

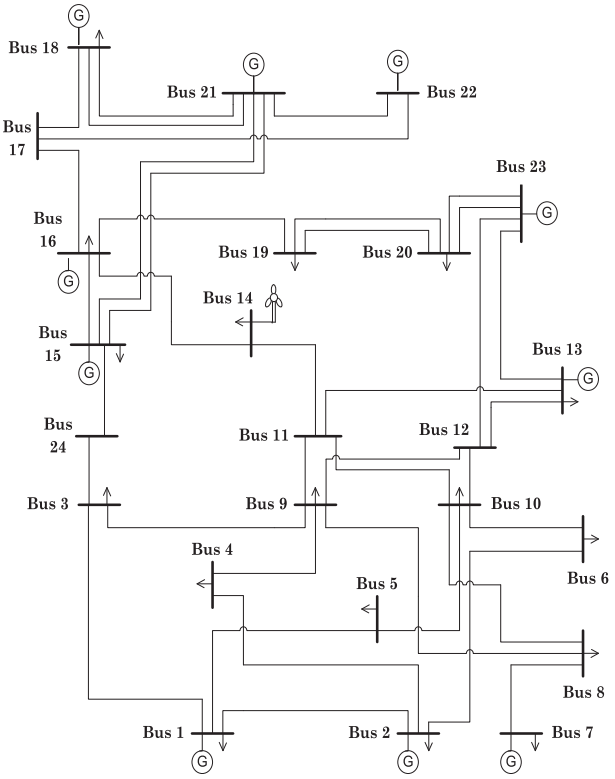

Fig. 3. Modified IEEE 24-bus test system.

as WF's CF. The capacity factor of a wind farm is an appropriate parameter that could be used to estimate expected output power of the WF. When the spatial distribution of wind speed over a WF is ignored, the CF of a single WT and that of a WF with a specified number of installed same WTs would be equal. However, considering wind speed's spatial distribution leads to the WF's CF be different with a single WT's CF.

The CF of a single WT could be calculated as follows:

1. Generate W wind speed values by applying the Monte Carlo Simulation (MCS) method to the Weibull distribution; i.e., $V_w\ ;\ w = 1,\ 2,\ \ldots, W$, where W equals to 8760
2. By applying V_w to the WT's power curve, its output power (P_w) could be calculated.
3. The capacity factor of the wind turbine would be equal to:

$$CF_{WT} = \frac{\sum_{w=1}^{W} P_w}{W \times rated\ power\ of\ the\ WT} \tag{1}$$

To calculate the CF of a WF with N numbers of same WTs installed considering the spatial distribution of wind speed, the following steps should be taken after step 1:

4. For each V_w, generate N values by applying MCS to the Poisson distribution. Consequently, there would be $W \times N$ wind speed values as $V_{w,n}$.
5. By applying $V_{w,n}$ to the WT's power curve, the output power of each WT could be calculated; i.e., $P_{w,n}$.
6. The output power of the WF, i.e. $P_w^{WF}\mathrm{P_{ws}^{WF}}$, could be calculated as follows:

$$P_w^{WF} = \sum_{n=1}^{N} P_{w,n} \tag{2}$$

7. The capacity factor of the wind farm would be equal to:

$$CF_{WF} = \frac{\sum_{w=1}^{W} P_w^{WF}}{W \times (N \times rated\ power\ of\ the\ WT)} \tag{3}$$

Fig. 1 shows the CF of a single WT and a WF with different numbers of installed WTs, considering spatial distribution of wind speed. For this purpose, the main statistical characteristics of actual wind speed data in three different sites [29], Table 1, and the power curve of a 2-MW wind turbine (Vestas V80/2000) [30] are used.

According to Fig. 1, the following results are obtained:

1. The capacity factor of a WF is less than that of a single WT.
2. In a WF, when the number of installed WTs exceeds a certain limit (50 for example), the capacity factor does not change and can be assumed to be constant.

2.2. Load model

Load uncertainty is modeled in the proposed method via different scenarios. In this way, it is assumed that load scenarios and their occurrence probabilities are predetermined. In other words, different load levels have been used to model the load uncertainty instead of using just one load level. As an example, these scenarios could be divided into the *low load*, *middle load*, and *peak load* levels with specified probabilities. Assuming ls to be the index of different load scenarios, $ld_{t,i,ls}$ $\mathrm{D_{t,i,ls}}$will show the level of demand in the t^{th} planning horizon, i^{th} bus number, and ls^{th} scenario, which has an occurrence probability of $\alpha_{ls}\ ;\ ls = 1,\ 2,\ \ldots, LS$.

2.3. The objective function of proposed TEP and GEP model

The objective function (OF) of the proposed method is to minimize the net present cost, which involves investment cost (C^{inv}), expected operation cost (EC^{ope}), and expected loss cost (EC^{loss}). If the planning horizon is divided into T periods, each of which containing ST subperiods, the cash flow diagram of the system planning is considered as Fig. 2. Here, it is assumed that the load is constant in each sub-period and the load growths in each period.

Investment cost is related to the total investment cost of the power system, which is the sum of the transmission network, thermal generation unit, and wind farm's investment costs. Expected operation cost consists of two parts: (1) the cost of generating electricity and (2) the cost of greenhouse gas emissions. To calculate the expected loss cost, the summation of total loss in all existent and invested lines is

Table 2
Candidate transmission line data for the IEEE-24 bus.

Line no.	From	To	Circuit length (km)	Voltage level (kV)	Capacity (MW)	R (pu)	X (pu)	Investment cost (M$)
CL_1	1	8	35	132	175	0.0348	0.1344	3.01
CL_2	2	8	33	132	175	0.0328	0.1267	2.84
CL_3	6	7	50	132	175	0.0497	0.1920	4.31
CL_4	13	14	31	230	500	0.0057	0.0447	4.58
CL_5	14	23	43	230	500	0.0080	0.0620	6.35
CL_6	16	23	57	230	500	0.0105	0.0822	8.41
CL_7	19	23	42	230	500	0.0078	0.0606	6.20

Table 3
Candidate generation unit data for the IEEE-24 bus.

Unit no.	Bus no.	Unit capacity (MW)	Technology	Emission rate (ton/MWh)	Operation cost ($/MWh)	Investment cost (M$)
CU_1–CU_3	1	20	Combined cycle	0.4881	46.52	14.9
CU_4–CU_6	1	76	Coal	0.9654	25.44	205
CU_7–CU_9	2	20	Combined cycle	0.4881	46.52	14.9
CU_{10}–CU_{12}	2	76	Coal	0.9654	25.44	205
CU_{13}–CU_{15}	7	100	Combined cycle	0.4881	47.61	75.1
CU_{16}–CU_{18}	13	197	Combined cycle	0.4881	46.85	148
CU_{19}–CU_{21}	15	12	Combined cycle	0.4881	45.41	8.96
CU_{22}–CU_{24}	15	155	Coal	0.9654	26.5	421
CU_{25}–CU_{27}	16	155	Coal	0.9654	26.5	421
CU_{28}–CU_{30}	18	400	Nuclear	0	13.03	1320
CU_{31}–CU_{33}	21	400	Nuclear	0	13.03	1320
CU_{34}–CU_{36}	23	155	Coal	0.9654	26.5	421
CU_{37}–CU_{39}	23	350	Coal	0.9654	26.5	951

Table 4
Different load scenarios.

Load scenario no.	LS1	LS2	LS3
Percentage of peak load (%)	100	66.94	33.88
Occurrence probability (%)	6.96	64.85	28.19

Table 5
Candidate wind farm data for the IEEE-24 bus.

WF no.	Bus no.	Wind speed characteristics	Capacity factor of the WF		Investment cost (M $/MW)
			With spatial distribution of wind speed	Without spatial distribution of wind speed	
CWF_1	1	North Battleford	0.50	0.55	1,601,328
CWF_2	3	Swift Current	0.54	0.60	1,602,242
CWF_3	8	Toronto	0.51	0.57	1,603,613
CWF_4	18	North Battleford	0.50	0.55	1,602,790
CWF_5	20	Swift Current	0.54	0.60	1,607,178

multiplied by constant value CL_t^{pu} as the cost of per unit loss [31].

2.4. Probabilistic optimal power flow

In the proposed TEP and GEP model, according to the uncertainties associated with WF output power and load, probabilistic optimal power flow (OPF) should be used instead of the conventional OPF. Monte Carlo Simulation (MCS), used in the present work, is one of the most common and accurate stochastic methods [32].

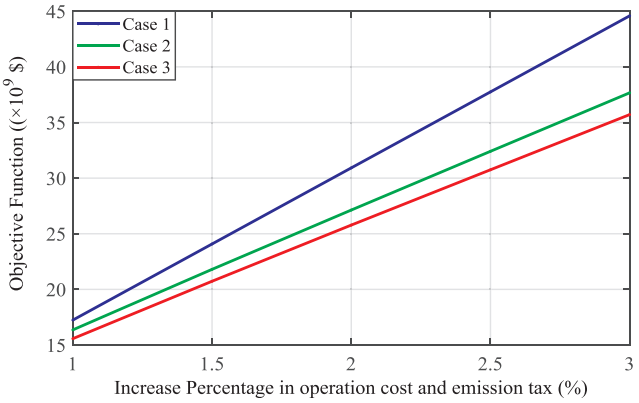

Fig. 4. Objective function values for different increase percentages in operation costs of thermal generators and CO_2 emission tax (wind power limitation is 500 MW in each node).

3. Problem formulation

Objective function formulation of the proposed TEP and GEP model in the presence of wind power and its constraints are presented and discussed in this section. Net present cost of the power system planning can be calculated as follows:

Table 6
Expansion plans for the three cases in the planning horizon.

		T_1	T_2	T_3
Transmission expansion planning	Case 1	CL_1, CL_3, CL_5, CL_7	CL_2, CL_4	–
	Case 2	CL_3, CL_5, CL_7	CL_1, CL_2, CL_4	–
	Case 3	CL_1, CL_3, CL_5, CL_7	CL_6	CL_2
Generation expansion planning	Case 1	CU_1, CU_2, CU_3, CU_7, CU_8, CU_9, CU_{13}	CU_{14}, CU_{16}, CU_{17}, CU_{19}, CU_{20}, CU_{28}	CU_4, CU_5, CU_6, CU_{10}, CU_{11}, CU_{15}, CU_{18}, CU_{22}, CU_{25}, CU_{26}
	Case 2	–	CU_7, CU_{16}, CU_{28}	CU_1, CU_2, CU_3, CU_4, CU_8, CU_9, CU_{10}, CU_{11}, CU_{12}, CU_{13}, CU_{14}, CU_{15}, CU_{17}, CU_{18}, CU_{19}, CU_{20}, CU_{21}
	Case 3	–	CU_7, CU_8, CU_9, CU_{28}	CU_1, CU_2, CU_3, CU_{10}, CU_{11}, CU_{13}, CU_{14}, CU_{15}, CU_{16}, CU_{17}, CU_{18}, CU_{19}, CU_{20}
Wind farm expansion planning	Case 2	$N_{cwf1,1,T1} = 7$, $N_{cwf2,3,T1} = 10$, $N_{cwf3,8,T1} = 10$, $N_{cwf5,20,T1} = 10$	–	–
	Case 3	$N_{cwf1,1,T1} = 5$, $N_{cwf2,3,T1} = 10$, $N_{cwf3,8,T1} = 10$, $N_{cwf5,20,T1} = 10$	$N_{cwf1,1,T2} = 5$	–
Objective function ($\times 10^9$ $)	Case 1	17.24		
	Case 2	16.36		
	Case 3	15.57		

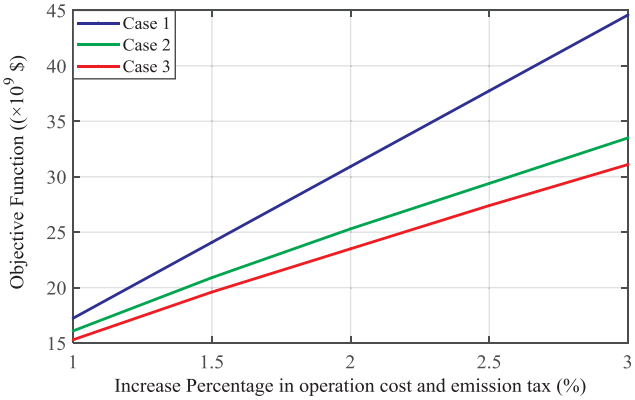

Fig. 5. Objective function values for different increase percentages in operation costs of thermal generators and CO_2 emission tax (wind power limitation is 1000 MW in each node).

Table 7
Objective function values ($\times 10^9$ $) and the difference between Cases 2 and 3.

Increase percentage in operation cost and CO_2 emission tax (%)		1	1.5	2	2.5	3
Wind power limitation is 500 MW in each node	Case 1	17.24	24.08	30.92	37.75	44.59
	Case 2	16.36	21.8	27.13	32.41	37.67
	Case 3	15.57	20.73	25.78	30.75	35.71
	Overestimation in Case 3 (%)	4.83	4.91	4.98	5.12	5.20
Wind power limitation is 1000 MW in each node	Case 1	17.24	24.08	30.92	37.75	44.59
	Case 2	16.14	20.93	25.25	29.39	33.52
	Case 3	15.27	19.63	23.53	27.35	31.11
	Overestimation in Case 3 (%)	5.39	6.21	6.81	6.94	7.19

Table 8
Candidate transmission line data for the IEEE-118 bus.

Line no.	From	To	Circuit length (km)	Capacity (MW)	R (pu)	X (pu)	Investment cost (M$)
CL_1	11	13	65	700	0.0223	0.0731	13.73
CL_2	35	37	80	700	0.0110	0.0497	16.90
CL_3	49	54	60	700	0.0869	0.2910	12.67
CL_4	56	59	55	700	0.0803	0.2390	11.61
CL_5	61	62	60	700	0.0082	0.0376	12.67
CL_6	49	66	50	700	0.0180	0.0919	10.56
CL_7	89	90	70	700	0.0238	0.0997	14.78
CL_8	34	37	100	600	0.0026	0.0094	21.12
CL_9	70	71	90	800	0.0088	0.0355	19.00
CL_{10}	65	68	80	700	0.0014	0.0160	16.90
CL_{11}	30	38	75	700	0.0046	0.0540	15.84

Table 10
Candidate wind farm data for the IEEE-118 bus.

WF no.	Bus no.	Wind speed characteristics	Capacity factor of the WF		Investment cost (M $/MW)
			With spatial distribution of wind speed	Without spatial distribution of wind speed	
CWF_1	42	North Battleford	0.50	0.55	1,601,328
CWF_2	1	North Battleford	0.50	0.55	1,601,328
CWF_3	54	North Battleford	0.50	0.55	1,601,328
CWF_4	40	North Battleford	0.50	0.55	1,601,328
CWF_5	56	North Battleford	0.50	0.55	1,601,328
CWF_6	59	North Battleford	0.50	0.55	1,601,328
CWF_7	61	North Battleford	0.50	0.55	1,601,328
CWF_8	65	Swift Current	0.54	0.60	1,602,242
CWF_9	69	Swift Current	0.54	0.60	1,602,242
CWF_{10}	74	Swift Current	0.54	0.60	1,602,242
CWF_{11}	90	Swift Current	0.54	0.60	1,602,242
CWF_{12}	91	Swift Current	0.54	0.60	1,602,242
CWF_{13}	62	Swift Current	0.54	0.60	1,602,242
CWF_{14}	116	Swift Current	0.54	0.60	1,602,242
CWF_{15}	34	Toronto	0.51	0.57	1,603,613
CWF_{16}	36	Toronto	0.51	0.57	1,603,613
CWF_{17}	46	Toronto	0.51	0.57	1,603,613
CWF_{18}	104	Toronto	0.51	0.57	1,603,613
CWF_{19}	105	Toronto	0.51	0.57	1,603,613
CWF_{20}	110	Toronto	0.51	0.57	1,603,613
CWF_{21}	112	Toronto	0.51	0.57	1,603,613

$$
\begin{aligned}
Min \Big\{ & \sum_{t=1}^{T} \frac{1}{(1+dr)^{(t-1)\times ST}} \Big[\sum_{cl=1}^{CL} \left((ul_{t,cl} - ul_{(t-1),cl}).\ C_{t,cl}^{LI} \right) + \\
& \sum_{i=1}^{N} \Big(\sum_{ctg=1}^{CTG} \left((ug_{i,t,ctg} - ug_{i,(t-1),ctg}).\ C_{t,ctg}^{TGI} \right) \\
& + \sum_{cwf=1}^{CWF} \left((N_{i,t,cwf}^{WB} - N_{i,(t-1),cwf}^{WB}).\ C_{t,cwf}^{WBI} \right) \Big) \Big] + \\
& \sum_{t=1}^{T} \frac{8760 \times ST}{(1+dr)^{(t-1)\times ST}} \Big[\sum_{i=1}^{N} \sum_{ls=1}^{LS} (\alpha_{ls}) \times \\
& \Big(\sum_{etg=1}^{ETG} (OC_{etg} + ETax \times ER_{etg}).\ P_{i,t,etg,ls} \\
& + \sum_{ctg=1}^{CTG} (OC_{ctg} + ETax \times ER_{ctg}).\ P_{i,t,ctg,ls} \Big) \Big] + \\
& \sum_{t=1}^{T} \frac{8760 \times ST}{(1+dr)^{(t-1)\times ST}} \Big[\sum_{i=1}^{N} \sum_{ls=1}^{LS} \alpha_{ls}.\ CL_t^{pu}. \\
& \left(\sum_{el=1}^{EL} P_{el,t,ls}^{loss} + \sum_{cl=1}^{CL} P_{cl,t,ls}^{loss} \right) \Big] \Big\}
\end{aligned}
\tag{4}
$$

As can be seen, the objective function consists of three main terms. The first term is the total investment cost. $ul_{t,cl}$ represents the decision

Table 9
Candidate generation unit data for the IEEE-118 bus.

Unit no.	Bus no.	Unit capacity (MW)	Technology	Emission rate (ton/MWh)	Operation cost ($/MWh)	Investment cost ($\times 10^8$ $)
CU_1–CU_4	4	250	Nuclear	0	10.27	7.69
CU_5–CU_8	8	250	Nuclear	0	12.33	7.70
CU_9–CU_{12}	107	250	Nuclear	0	13.03	7.71
CU_{13}–CU_{16}	25	250	Combined cycle	0.4881	45.41	1.74
CU_{17}–CU_{20}	40	250	Combined cycle	0.4881	46.52	1.74
CU_{21}–CU_{24}	56	250	Combined cycle	0.4881	47.61	1.75
CU_{25}–CU_{28}	62	250	Combined cycle	0.4881	46.85	1.75
CU_{29}–CU_{32}	85	250	Combined cycle	0.4881	48.23	1.74
CU_{33}–CU_{36}	66	250	Coal	0.9654	25.44	6.29
CU_{37}–CU_{40}	78	250	Coal	0.9654	26.50	6.33

Table 11
Expansion plans for the three cases in the planning horizon (IEEE 118-bus).

		T_1
Transmission expansion planning	Case 1	CL_1, CL_5, CL_7, CL_{10}
	Case 2	CL_2, CL_7, CL_9, CL_{10}
	Case 3	CL_5, CL_6, CL_{10}, CL_{11}
Generation expansion planning	Case 1	CU_1, CU_2, CU_5, CU_6, CU_7, CU_9, CU_{10} CU_{13}, CU_{17}, CU_{18}, CU_{21}, CU_{22}, CU_{23}, CU_{25} CU_{26}, CU_{27}, CU_{28}, CU_{29}, CU_{30}, CU_{31}, CU_{37}
	Case 2	CU_1, CU_5, CU_6, CU_7, CU_9, CU_{17}, CU_{21} CU_{29}, CU_{30}, CU_{37}
	Case 3	CU_1, CU_5, CU_6, CU_7, CU_9, CU_{29}
Total constructed wind farm capacity (MW)	Case 2	8800
	Case 3	10,500
Objective function ($\times 10^9$ \$)	Case 1	62.22
	Case 2	58.74
	Case 3	55.53

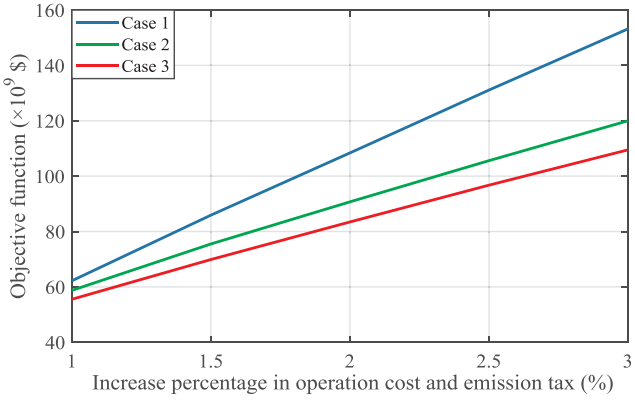

Fig. 6. Objective function values for different increase percentages in operation costs of thermal generators and CO_2 emission tax (wind power limitation is 600 MW in each node).

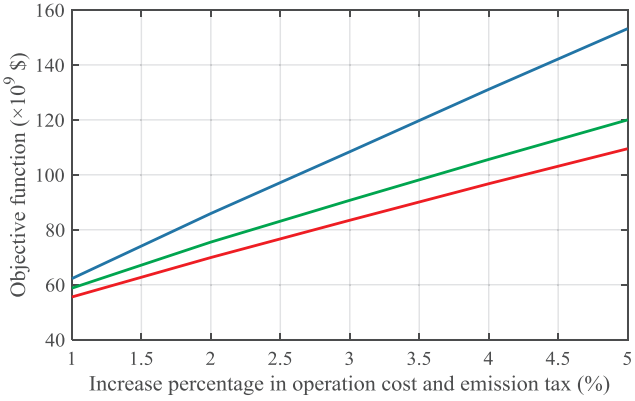

Fig. 7. Objective function values for different increase percentages in operation costs of thermal generators and CO_2 emission tax (wind power limitation is 1000 MW in each node).

variable of constructing the cl^{th} candidate line in the t^{th} planning time interval. It is supposed that when $ul_{(t-1),cl}$ is equal to 1, also $ul_{t,cl}$ should be equal to 1. In this way, the cost of the cl^{th} candidate line construction is considered only once. This is also true for investment decision variable of thermal generators ($ug_{i,t,ctg}$) and wind farms ($N^{WB}_{i,t,cwf}$). These constraints could be applied to the proposed model as follows:

Table 12
Objective function values ($\times 10^9$ \$) and the difference between Case 2 and 3 (IEEE 118-bus).

Increase percentage in operation cost and CO_2 emission tax (%)		1	1.5	2	2.5	3
Wind power limitation is 600 MW in each node	Case 1	62.22	85.92	108.4	131.1	153.2
	Case 2	58.74	75.51	90.72	105.6	120.0
	Case 3	55.53	69.89	83.46	96.75	109.5
	Overestimation in Case 3 (%)	5.46	7.43	8.00	8.38	8.75
Wind power limitation is 1000 MW in each node	Case 1	62.22	85.92	108.4	131.1	153.2
	Case 2	58.57	70.57	79.49	87.80	95.87
	Case 3	54.14	63.32	70.87	77.46	83.84
	Overestimation in Case 3 (%)	7.56	10.27	10.84	11.78	12.55

$$ul_{t,cl} \geqslant ul_{(t-1),cl} \tag{5}$$

$$ug_{i,t,ctg} \geqslant ug_{i,(t-1),ctg} \tag{6}$$

$$N^{WB}_{i,t,cwf} \geqslant N^{WB}_{i,(t-1),cwf} \tag{7}$$

$$ul_{0,cl} = 0 \tag{8}$$

$$ug_{i,0,ctg} = 0 \tag{9}$$

$$N^{WB}_{i,0,cwf} = 0 \tag{10}$$

$N^{WB}_{i,t,cwf}$ is an integer variable that shows the number of WT blocks that should be installed in candidate wind farm cwf in the i^{th} bus at t^{th} planning time interval. The capacity of each block is supposed to be specified. In the proposed model, it is possible to construct any type of thermal generation units as well as WT blocks in all buses. However, usually, there are some restrictions in this regard. For example, there may be a limitation that nuclear power plants should only be constructed in a specified bus or wind farms could be built in some limited buses. These limitations can be considered by adding relevant constraints to the model.

The second term of the objective function represents expected operation cost, which consists of two parts. The first part, which relates to the fuel consumption, is expressed as a multiplication of the generator unit's output power at its operation cost. The second part is based on global concerns of greenhouse gas emissions and CO_2 release taxes, which is characterized by the multiplication of three terms, generator unit's output power, CO_2 emission rate, and emission tax. For the sake of simplicity, the discount rate coefficient is only applied to the expected operation cost of each period.

The last term shows expected loss cost of transmission lines. Here, also the discount rate coefficient is only applied to the expected loss cost of each period. To calculate power losses of existent and invested lines, suppose $ELPF_{t,i,j,ls}$ and $CLPF_{t,i,j,ls}$ to be active power flow from bus i to j in existent and invested lines, respectively, and voltage magnitude of all buses equals to 1 pu. Then, total power loss can be calculated as follows:

$$\sum_{el=1}^{EL} P^{loss}_{el,t,ls} = \frac{1}{2} \times \sum_{i=1}^{N} \sum_{j=1}^{N} (ELPF_{t,ij,ls}) \tag{11}$$

$$\sum_{cl=1}^{CL} P^{loss}_{cl,t,ls} = \frac{1}{2} \times \sum_{i=1}^{N} \sum_{j=1}^{N} (CLPF_{t,ij,ls}) \tag{12}$$

$$ELPF_{t,ij,ls} = -B_{ij}.\ Sin(\delta_{t,ij,ls}) + G_{ij}(1-Cos(\delta_{t,ij,ls})) \tag{13}$$

$$CLPF_{t,ij,ls} = ul_{t,cl}.\ (-B_{ij}.\ Sin(\delta_{t,ij,ls}) + G_{ij}(1-Cos(\delta_{t,ij,ls}))) \tag{14}$$

$$\delta_{t,ij,ls} = \delta_{t,i,ls} - \delta_{t,j,ls} \tag{15}$$

As can be noted, Eqs. (13) and (14) are nonlinear. To linearize them,

$\mathrm{Sin}(\delta_{t,ij,ls})$ is simplified to $\delta_{t,ij,ls}$ and $\mathrm{Cos}(\delta_{t,ij,ls})$ is reformulated using Special Ordered Set of Type 2 (SOS2) [33,34]. In addition, Eq. (14) is reformulated as follows:

$$-ul_{t,cl}.\ M \leqslant CLPF_{t,ij,ls} - (-B_{ij}.\ Sin(\delta_{t,ij,ls}) + G_{ij}(1 - Cos(\delta_{t,ij,ls}))) \leqslant ul_{t,cl}.\ M \tag{16}$$

where M is a big constant value.

In addition to the constraints presented in Eqs. (5)–(10), the following constraints are considered in the proposed MILP model:

$$\sum_{etg=1}^{ETG} P_{etg,i,t,ls} + \sum_{ctg=1}^{CTG} P_{ctg,i,t,ls} + \sum_{cwf=1}^{CWF} P_{cwf,i,t,ls} - d_{t,i,ls} = \sum_{\substack{j=1 \\ j\neq i}}^{N} ELPF_{t,ij,ls} + \sum_{\substack{j=1 \\ j\neq i}}^{N} CLPF_{t,ij,ls} \tag{17}$$

$$ELPFlow_{t,ij,ls} \leqslant ELCap_{\max,ij} \tag{18}$$

$$CLPFlow_{t,ij,ls} \leqslant ul_{t,cl} \times CLCap_{\max,ij} \tag{19}$$

$$ETGCap_{\min,i,etg} \leqslant P_{etg,i,t,ls} \leqslant ETGCap_{\max,i,etg} \tag{20}$$

$$ug_{i,t,ctg}.\ CTGCap_{\min,i,ctg} \leqslant P_{ctg,i,t,ls} \leqslant ug_{i,t,ctg}.\ CTGCap_{\max,i,ctg} \tag{21}$$

$$P_{cwf,i,t,ls} \leqslant CF_{cwf} \times N^{WB}_{cwf,i,t} \times WBC \tag{22}$$

$$\delta_{\min,i} \leqslant \delta_{t,i,ls} \leqslant \delta_{\max,i} \tag{23}$$

Eq. (17) represents active balance at all buses. Capacity limitations of existent and candidate lines and thermal generator units are considered by (18)–(21). WF's output power limitation and voltage angle constraints of each bus are considered by (22) and (23), respectively.

4. Illustrative results

In this section, two test systems namely IEEE 24-bus Reliability Test System (RTS) and IEEE 118-bus are studied and the simulation results are demonstrated. All numerical studies are run using CPLEX [35] solver within the General Algebraic Modeling System (GAMS) [36] environment on a computer with Sony Core i5 CPU and 4 GB of RAM. In both test systems, the following common assumptions are considered:

1. No new buses are added to the power system.
2. The power curve of a 2-MW wind turbine (Vestas V80/2000) [30] is used to calculate the output power of the WT.
3. Weibull and Poisson distributions are used to model temporal and spatial distributions of wind speed over the wind farm.
4. In the real-world applications, places with the highest wind intensity can be chosen as candidate places to build the wind farm. However, since we deal with test systems here, the candidate buses for WF installation are considered to be known.

4.1. IEEE 24-bus

Fig. 3 illustrates the single diagram of the IEEE 24-bus test system, which comprises 24 buses, 32 existing generation units, 34 existing transmission lines, and 17 load centers with 2850 MW as the peak load [37].

Table 2 provides candidate transmission lines data, which obtained from [38]. It is assumed that to expand the generation capacity, all types of existing generation units except hydro units can be added up to 3 units. The operation and investment costs, as well as CO_2 emission rates of each generation unit type, are given in Table 3 based on [4,39]. The operation costs and emission rate values shown in the table are used also for the existing generation units.

Three periods, five years each, are considered for the 15-year planning horizon. The peak load value in each period is considered to be constant. Also, the load growth rate per stage is equal to 25%. The peak load value in the first period is 1.25 times the base system. Table 4 shows the load scenarios and their occurrence probabilities. Table 5 provides investment costs [39] and locations through the system of wind farms to be constructed.

Wind power is available in 50-MW blocks and the maximum wind power that can be built in each node is equal to 500 MW. The value of CL_t^{pu} is equal to 150 $/MWh while CO_2 emission tax is equal to 45 $/ton.

To see how spatial distribution of wind speed affects the power system expansion planning, three following cases were analyzed:

1. Case 1: Power system expansion planning without wind power penetration
2. Case 2: Power system expansion planning in the presence of wind power considering the spatial distribution of wind speed
3. Case 3: Power system expansion planning in the presence of wind power without considering the wind speed's spatial distribution

Table 6 provides the expansion plans for the three cases in the planning horizon. As can be seen, the value of the objective function in Case 1 is 17.24×10^9 $, which is 5.1% higher than that of Case 2. In other words, penetration of wind farm makes the objective function to decrease. The noteworthy point in this regard is that ignoring wind speed's spatial distribution, i.e. in Case 3, not only changes the plan but also makes the planner expect a further reduction in the value of objective function. The reason for this result is taking into account the capacity factor of a single wind turbine instead of the wind farm's capacity factor, which itself leads to overestimation in wind power expectation and 4.8% more reduction in expected objective function value than Case 2.

Considering the limitations in fossil fuel resources and environmental concerns about greenhouse gas emissions, an increase may occur in operation cost of thermal generation units and/or CO_2 emission taxes, leading to a growing tendency in using renewable energies. In this way, disregarding wind speed's spatial distribution over the wind farm may lead to more overestimation in expected objective function value. To show this result, the values of the expected objective function are presented in Fig. 4 for different values of the increase in the CO_2 emission tax and operation costs of thermal generation units. As can be seen, with the increase in fuel prices and emission taxes, the difference between the objective functions of Cases 2 and 3 would be greater, suggesting a more overestimation in expected objective function value.

This overestimation would be even more if there is the possibility of building wind farms with more capacity in the power system. As shown in Fig. 5, it is assumed that the maximum allowable wind power in each node is equal to 1000 MW.

As expected, with an increase in the possibility of further development of wind resources, disregarding wind speed's spatial distribution, i.e. Case 3, leads to a more overestimation in the expected objective function.

Table 7 presents the values of the objective function and the difference between those of Cases 2 and 3 in the conditions mentioned above.

4.2. IEEE 118-bus

IEEE 118-bus test system is also used to show how spatial distribution of wind speed over a WF could affect the expansion planning of the power system. IEEE 118-bus power system comprises 54 thermal generating units, 99 loads, and 186 transmission lines. All data on the existing generation units and transmission lines are given in MATPOWER 6 package [40], where the capacity of transmission lines was considered to be 700 MW. The data of candidate transmission lines, generation units, and WFs are shown in Tables 8–10, which are

obtained from [39]. The data of load distribution in the planning horizon are also the same as those presented in [39].

One period is considered for the planning horizon, which is 10 years. Wind power is available in 100-MW blocks and the maximum wind power that can be built in each node is equal to 600 MW. The rest of the data are the same as those in Section 4.1.

Table 11 provides the expansion plans for the three cases in the planning horizon. As can be seen, the value of the objective function in Case 1 is 62.22×10^9 $, which is 5.6% higher than Case 2. Accordingly, the penetration of wind farm into the power system may be profitable. However, ignoring wind speed's spatial distribution, i.e. in Case 3, again changes the optimal plan and the expected objective function. The results show that disregarding the spatial distribution of wind speed makes 5.46% extra reduction in the expected objective function than Case 2, which is not favorable in the viewpoint of the planner and wind farm owner.

Fig. 6 shows that how different values of the increase in the CO_2 emission tax and operation costs of thermal generation units can affect the values of the expected objective function. Moreover, Fig. 7 shows the same results assuming that the maximum allowable wind power in each node is equal to 1000 MW.

As expected, with an increase in the CO_2 emission tax and operation costs of thermal generation units and in the possibility of further development of wind resources, disregarding wind speed's spatial distribution, i.e. Case 3, leads to more overestimation in the expected objective function. Table 12 shows the values of the objective function and the differences between those of Cases 2 and 3 in the conditions mentioned above.

5. Conclusions

In this paper, a MILP model is proposed for the simultaneous GEP and TEP modeling of power systems with the presence of wind power to show how wind speed's spatial distribution over a wind farm affects the plan and expected objective function. To model the temporal and spatial distribution of wind speed, Weibull and Poisson distributions are used, respectively. Wind farm's capacity factor is used to model its output power and different load scenarios are used to consider the uncertainty on demand value. Probabilistic DC OPF using MCS technique is applied to the proposed model and the total cost (i.e., investment cost, operation cost, and loss cost) are formulated as the objective function of the presented expansion model. Operation cost involves the cost of electric power generation and CO_2 emission tax, which are related to the thermal generation units.

First, it has been shown that considering the spatial distribution of wind speed leads to the capacity factor of a wind farm to be different from that of a single wind turbine. To deal with this situation, the power curve of a 2-MW wind turbine (Vestas V80/2000) and the main statistical characteristics of actual wind speed data in three different sites are used. However, it is observed that the capacity factor of a wind farm with a threshold number of installed wind turbines remains constant and the addition of extra wind turbines does not change its capacity factor. Furthermore, it is exposed that ignoring wind speed's spatial distribution makes overestimation in the expected wind power of the wind farms; i.e., the wind farm owner expects more electric power than what happens in the reality. As a result, it affects the optimal plan of power system expansion and the expected objective function value. In other words, since the expected output power of the wind farm is overestimated, the planner expects less cost. Finally, it is found that the higher the share of wind power in load supplying is, the greater the overestimation on the wind farm's output power expectation would be. As an example, an increase may occur in the operation cost of thermal generation units due to the limitations of fossil fuel resources. Alternatively, regarding the environmental concerns about greenhouse gas emissions, the CO_2 emission taxes may increase. Then again, there would be the possibility of building wind farms with more capacity in the power system. Certainly, in all cases mentioned above, the tendency to use more renewable energy, including wind, will increase. Consequently, disregarding wind speed's spatial distribution leads to more overestimation in the expected objective function.

References

[1] Wang X, McDonald JR. Modern power system planning. New York: McGraw-Hill; 1994.
[2] Seifi H, Sepasian MS. Electric power system planning, issues, algorithms and solutions. Springer; 2011.
[3] Rouhani A, Hosseini SH, Raoofat M. Composite generation and transmission expansion planning considering distributed generation. Int J Electr Power Energy Syst 2014;62:792–805.
[4] Park H, Baldick R. Stochastic generation capacity expansion planning reducing greenhouse gas emissions. IEEE Trans Power Syst 2015;30(2):1026–34.
[5] Ugranlı F, Karatepe E. Multi-objective transmission expansion planning considering minimization of curtailed wind energy. Int J Electr Power Energy Syst 2015;65:348–56.
[6] Li J, Ye L, Zeng Y, Wei H. A scenario-based robust transmission network expansion planning method for consideration of wind power uncertainties. CSEE J Power Energy Syst 2016;2(1):11–8.
[7] Conradsen K, Nielsen LB, Prahm LP. Review of Weibull statistics for estimation of wind speed distributions. J Clim Appl Meteorol 1984;23:1173–83.
[8] Brown BG, Katz RW, Murphy AH. Time series models to simulate and forecast wind speed and wind power. J Clim Appl Meteorol 1984;23:1184–95.
[9] Yesilbudak M, Sagiroglu S, Colak I. A new approach to very short term wind speed prediction using k-nearest neighbor classification. Energy Convers Manage 2013;69:77–86.
[10] Lei M, Shiyan L, Chuanwen J, Hongling LL, Yan Z. A review on the forecasting of wind speed and generated power. Renew Sustain Energy Rev 2009;13:915–20.
[11] Velo RR, López P, Maseda F. Wind speed estimation using multilayer perceptron. Energy Convers Manage 2014;81:1–9.
[12] Gan L, Li G, Zhou M. Coordinated planning of large-scale wind farm integration system and transmission network. CSEE J Power Energy Syst 2016;2(1):19–29.
[13] Kamalinia S, Shahidehpour M. Generation expansion planning in wind-thermal power systems. IET Gen Trans Distrib 2010;4(8):940–51.
[14] Li C, Dong Z, Chen G, Luo F, Liu J. Flexible transmission expansion planning associated with large-scale wind farms integration considering demand response. IET Gen Trans Distrib 2015;9(15):2276–83.
[15] Orfanos GA, Georgilakis PS, Hatziargyriou ND. Transmission expansion planning of systems with increasing wind power integration. IEEE Trans Power Syst 2013;28(2):1355–62.
[16] Jabr RA. Robust transmission network expansion planning with uncertain renewable generation and loads. IEEE Trans Power Syst 2013;28(4):4558–67.
[17] Ugranli F, Karatepe E. Transmission expansion planning for wind turbine integrated power systems considering contingency. IEEE Trans Power Syst 2016;31(2):1476–85.
[18] Ugranli F, Karatepe E, Nielsen AH. MILP approach for bilevel transmission and reactive power planning considering wind curtailment. IEEE Trans Power Syst 2017;32(1):652–61.
[19] Dehghan S, Amjady N, Conejo AJ. Reliability-constrained robust power system expansion planning. IEEE Trans Power Syst 2016;31(3):2383–92.
[20] Rajesh K, Kannan S, Thangaraj C. Least cost generation expansion planning with wind power plant incorporating emission using differential evolution algorithm. Int J Electr Power Energy Syst 2016;80:275–86.
[21] Hemmati R, Hooshmand RA, Khodabakhshian A. Coordinated generation and transmission expansion planning in deregulated electricity market considering wind farms. Renew Energy 2016;85:620–30.
[22] Moradi M, Abdi H, Lumbreras S, Ramos A, Karimi Sh. Transmission Expansion Planning in the presence of wind farms with a mixed AC and DC power flow model using an Imperialist Competitive Algorithm. Electr Power Syst Res 2016;160:493–506.
[23] You Sh, Hadley SW, Shankar M, Liu Y. Co-optimizing generation and transmission expansion with wind power in large-scale power grids—implementation in the US Eastern Interconnection. Electr Power Syst Res 2016;133:209–18.
[24] Jadidoleslam M, Ebrahimi A, Latify MA. Probabilistic transmission expansion planning to maximize the integration of wind power. Renew Energy 2017;114:866–78.
[25] Zhan Y, Zheng QP, Wang J, Pinson P. Generation expansion planning with large amounts of wind power via decision-dependent stochastic programming. IEEE Trans Power Syst 2017;32:3015–26.
[26] Zolfaghari S, Riahy GHH, Abedi M. A new method to adequate assessment of wind farm's power output. Energy Convers Manage 2015;103:585–604.
[27] Reza Hemmati. Optimal design and operation of energy storage systems and generators in the network installed with wind turbines considering practical characteristics of storage units as design variable. J Clean Prod 2018;185:680–93.
[28] Sheen JN, Tsai MT, Wu SW. A benefits analysis for wind turbine allocation in a power distribution system. Energy Convers Manage 2013;68:305–12.
[29] Karki R, Hu P, Billinton R. A simplified wind power generation model for reliability evaluation. IEEE Trans Power Syst 2006;21(2):533–40.
[30] Motevasel M, Seifi AR. Expert energy management of a micro-grid considering wind energy uncertainty. Energy Convers Manage 2014;83:58–72.
[31] Sepasian MS, Seifi H, Akbari FA, Hatami AR. A multiyear security constrained

hybrid generation-transmission expansion planning algorithm including fuel supply costs. IEEE Trans Power Syst 2009;24(3):1609–18.
[32] Haque MH. Evaluation of power flow solutions with fixed speed wind turbine generating systems. Energy Convers Manage 2014;79:511–8.
[33] Beale E, Forrest J. Global optimization using special ordered sets. Math Program 1976;10:52–69.
[34] Anglani N, Oriti G, Colombini M. Optimized energy management system to reduce fuel consumption in remote military microgrids. Proc 8th IEEE Energy Convn Congress Exposition (ECCE) 2016.
[35] The ILOG CPLEX; 2008. [Online]. Available: < http://www.ilog.com/products/cplex > .
[36] Rosenthal RE. GAMS, A User's Guide. Washington, DC: GAMS Development Corporation; 2008.
[37] IEEE. Reliability test system task force of the application of probability methods subcommittee. Reliability test system. IEEE Trans Power App Syst 1979; PAS-;98(6):2047–54.
[38] Garcés LP, Conejo AJ, García-Bertrand R, Romero R. A bilevel approach to transmission expansion planning within a market environment. IEEE Trans Power Syst 2009;24(3):1523–622.
[39] Domínguez R, Conejo AJ, Carrión M. Toward fully renewable electric energy systems. IEEE Trans Power Syst 2015;30(1):316–26.
[40] Zimmerman RD, Murillo-Sánchez CE, Thomas RJ. MATPOWER: steady-state operations, planning and analysis tools for power systems research and education. IEEE Trans Power Syst 2011;26:12–9.